Supporting Information

Alcázar *et al.* 10.1073/pnas.0811734106

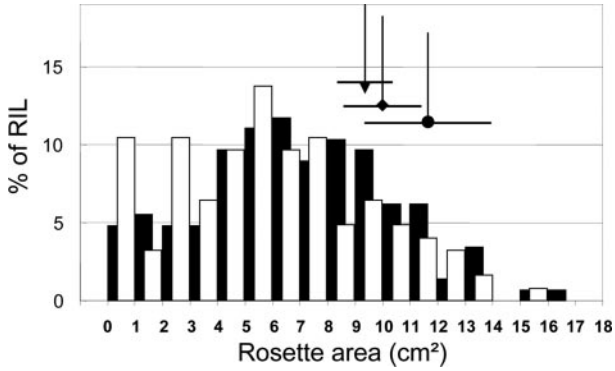

Fig. S1. Frequency distributions of rosette area from Ler × Kas-2 and L*er* × Kond RIL populations. The black and the white bars represent the percentage of RIL in the L*er* × Kas-2 and the L*er* × Kond populations, respectively. The value of the parental accessions L*er*, Kas-2, and Kond are shown (●, ▲, and ♦, respectively). The horizontal lines represent standard deviation.

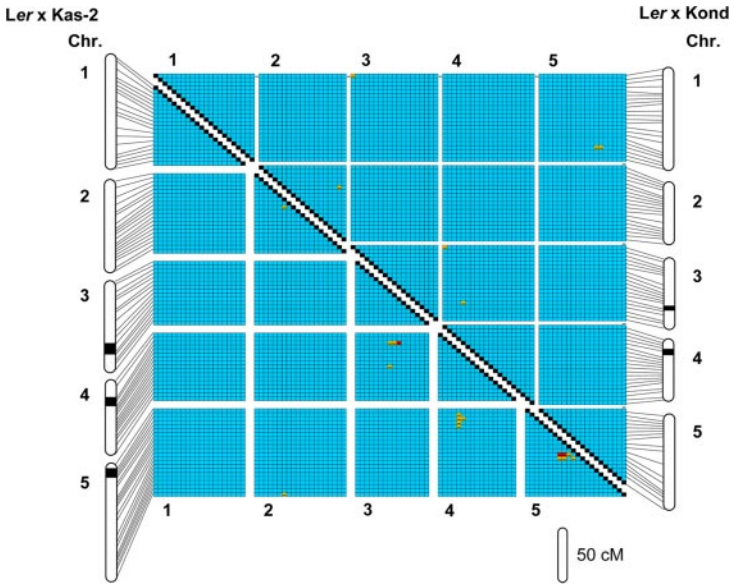

Fig. S2. Heat plot of the log likelihood ratio (LRR) from pairwise epistatic interactions detected by Epistat. (*Bottom Left* and *Top Right*) Heat plots for L*er* × Kas-2 and L*er* × Kond RILs, respectively. Genetic maps from each population are represented. Presence of epistatic interactions with an LLR >6 and >12 are indicated, respectively, in orange and red.

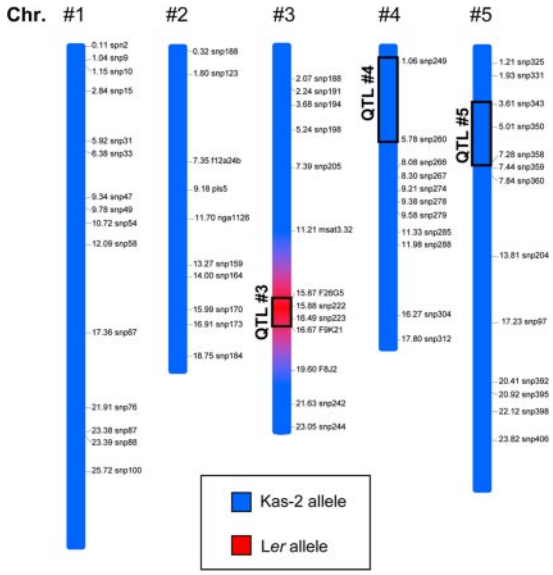

Fig. S3. Schematic representation of L*er* × Kas-2 NIL genotype. Each chromosome is represented in vertical bars. Markers and physical positions are shown. Kas-2 alleles are represented in blue and L*er* alleles in red. Positions of QTLs 3, 4, and 5 are indicated in boxes.

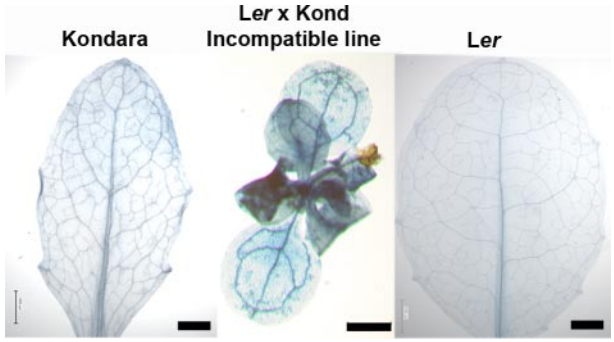

Fig. S4. Cell death phenotypes of incompatible L*er* × Kond lines. Spontaneous cell death was revealed by lactophenol TB staining of 3-week-old leaves of incompatible lines (*Middle*) and parental accessions (Kond, *Left*; L*er*, *Right*) grown at 14 °C.

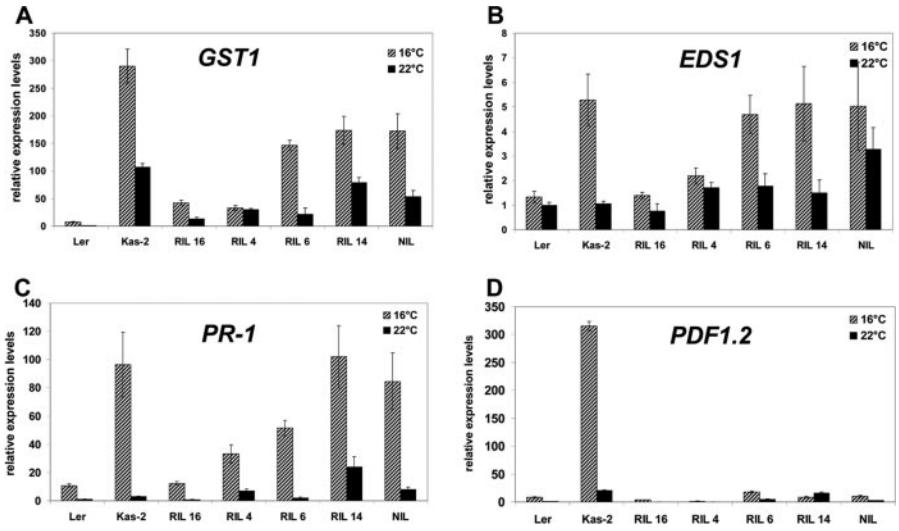

Fig. S5. Gene expression analyses. Transcript levels of *GST1* (*A*), *EDS1* (*B*), *PR-1* (*C*), and *PDF1.2* (*D*) in incompatible L*er* × Kas-2 RILs 4, 6, 14, and NIL; compatible L*er* × Kas-2 RIL 16; and parental lines grown at 14–16 °C (dashed) and 20–22 °C (black). Values were obtained by real-time PCR and are expressed relative to the level of transcripts in L*er* at 20 °C, which is assumed to be 1. Values are the mean ± SE of 3 replicates from 3 independent experiments.

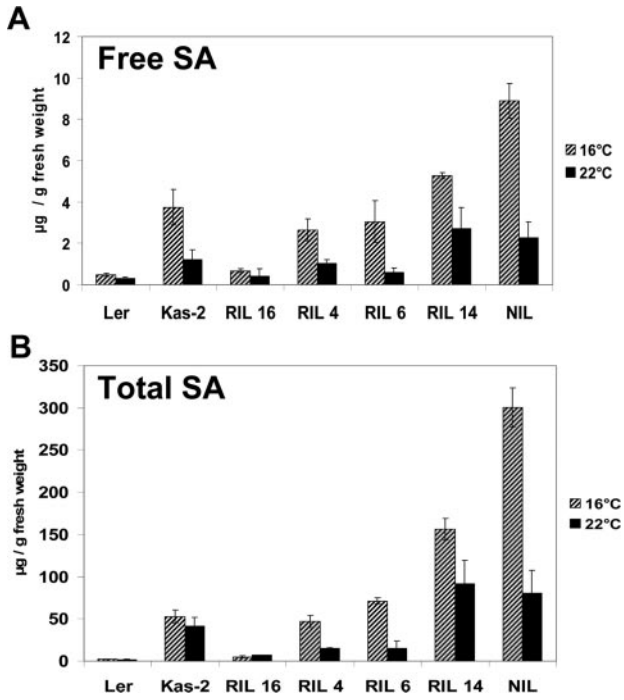

Fig. S6. Quantification of free (*A*) and total (*B*) salicylic acid levels in 3-week-old incompatible L*er* × Kas-2 RILs 4, 6, 14, and NIL; compatible L*er* × Kas-2 RIL 16; and parental lines grown at 14–16 °C (dashed) and 20–22 °C (black). Values presented are the mean ± SE of 3 biological replicates. These analyses were repeated twice in different batches of plants with similar results.

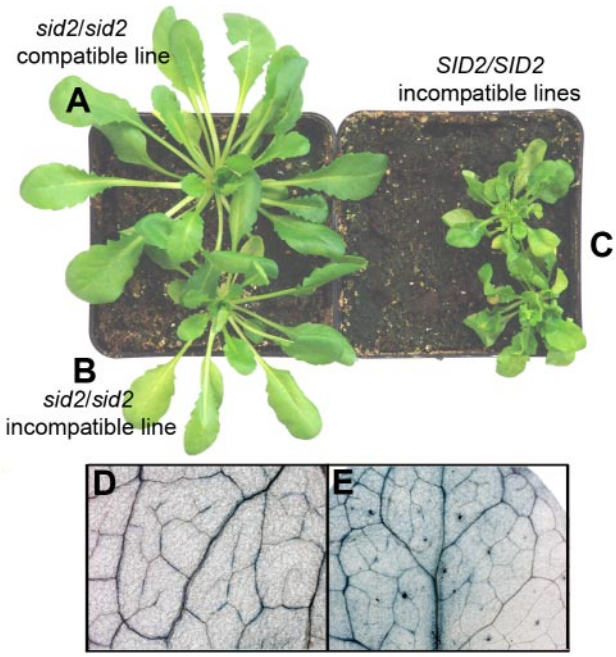

Fig. S7. Effect of the *Isochorismate synthase* mutation on phenotypes of incompatible L*er* × Kas-2 lines. Eight-week-old F_3 lines with different allele combinations were phenotyped at 14 °C. (*A*) Compatible line provided with *SID2* mutation (*sid2*/*sid2*, QTL 3: L*er*/L*er*, QTL 4: Col-0/Col-0, QTL 5: Kas-2/Kas-2). (*B*) Incompatible line provided with *SID2* mutation (*sid2*/*sid2*, QTL 3: L*er*/L*er*, QTL 4: Kas-2/Kas-2, QTL 5: Kas-2/Kas-2). (*C*) Incompatible lines provided with wild-type *SID2* gene (*SID2*/*SID2*, QTL 3: L*er*/L*er*, QTL 4: Kas-2/Kas-2, QTL 5: Kas-2/Kas-2). (*D*) TB staining of incompatible lines provided with *SID2* mutation or wild-type *SID2* gene (*E*).

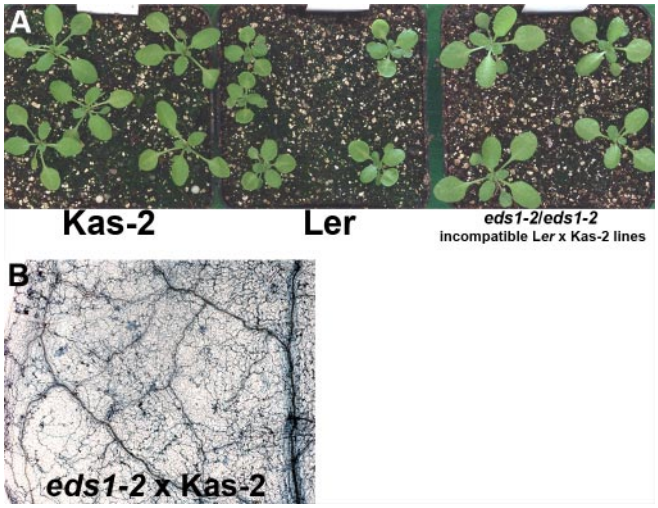

Fig. S8. Suppression of incompatible phenotypes by *EDS1* mutation. (*A*) Phenotype of 3-week-old *eds1–2* × Kas-2 lines harboring the incompatible allele interaction on QTL 3, QTL 4, and QTL 5 grown at 14 °C compared with parental lines L*er* and Kas-2. (*B*) Infection phenotype of *eds1–2* × Kas-2 incompatible lines. Two-week-old plants grown at 14 °C were inoculated with virulent *H. parasitica* isolate Cala2 and moved to 18 °C for optimal pathogen growth. Microscopic examination of TB-stained leaves to reveal dead plant cells and pathogen mycelium growth was performed 4 days postinoculation.

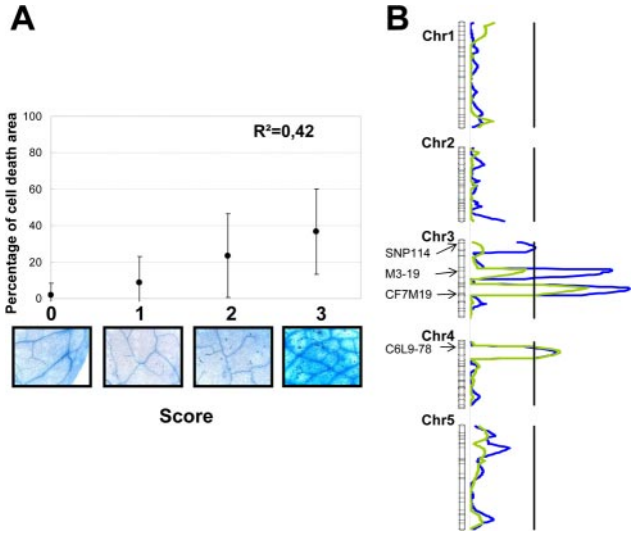

Fig. S9. Quantification of cell death. Cell death phenotype was measured using 2 different methods in the L*er* × Kas-2 RIL population. In the first method, the distribution of cell death was analyzed by microscopic visualization of lactophenol TB-stained leaves in 5-week-old plants grown at 14 °C. The same leaf from at least 3 different plants per line was used for these analyses. A value ranging from 0 to 3 was given to each RIL according to the following statements: 0, no visible cell death; 1, presence of isolated dead cells uniformly distributed in the leaf; 2, presence of small clumps of dead cells (up to 2 neighboring cells) uniformly distributed in the leaf; and 3, presence of necrotic areas (clumps of 3 or more cells) uniformly distributed in the leaf. This score was used for QTL detection of cell death. In an alternative method, the ratio between TB-stained area relative to total leaf area was measured using Image-Pro Analyzer (Media Cybernetics, Inc.) and used for QTL detection. Overall, the 2 quantification methods are correlated ($r^2 = 0.42$). Regardless of which method was used to quantify the extent of cell death, the same and significant QTLs ($P < 0.001$) were detected, except for the QTL on top chromosome 3 (snp114). For convenience, the scoring method was then used to quantify the extent of cell death in the L*er* × Kond RIL population (Fig. 1). (*A*) Correlation between the 2 methods used to quantify cell death after lactophenol TB staining of leaves. (*B*) LOD trace of QTL detection for the 2 independent quantification methods used to measure cell death. The LOD trace from the scoring method (blue) and for the percentage of cell death area (green) is shown. The black lines indicate the threshold of QTL detection determined by permutation test (LOD = 2.5). Markers close to detected QTL are indicated on the left side of the chromosomes.

Table S1. Segregation of incompatible phenotypes in F_2 populations derived from the cross between Landsberg *ERECTA* × Kas-2, L*er* × Uk-1, L*er* × Uk-3, Kas-2 × Uk-1, and Kas-2 × Uk-3 at 14 °C

F_2 population	No. of incompatible lines	Total no. plants	Model of dominance
Landsberg *ERECTA*♀ × Kas-2 ♂	8	250	3 loci (2 recessive + 1 dominant) χ^2 $P_{value} = 0.27$
L*er* ♀ × Uk-1 ♂	0	259	-
L*er* ♀ × Uk-3 ♂	0	264	-
Kas-2 ♀ × Uk-1 ♂	0	244	-
Kas-2 ♀ × Uk-3 ♂	0	204	-